

## Ab initio Structure Determination of Barium Periodate, $\text{Ba}_5\text{I}_2\text{O}_{12}$ , from Powder XRD Data

Frank Kubel,<sup>\*[a]</sup> Mariana Pantazi,<sup>[a]</sup> and Hans Hagemann<sup>[b]</sup>

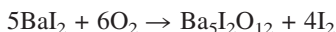
**Keywords:** X-ray diffraction; Barium periodate; Ab initio structure determination;

**Abstract.** The compound  $\text{Ba}_5\text{I}_2\text{O}_{12}$  was synthesized by heating a precipitate of dissolved  $\text{Ba}(\text{OH})_2 \cdot 8\text{H}_2\text{O}$  and  $\text{H}_5\text{IO}_6$ .  $\text{Rb}_2\text{O}$  was added to increase the crystallite size. The crystal structure was determined from conventional laboratory X-ray diffraction data by using a real-space structure solution approach followed by a Rietveld refinement. No constraints on positions were used. The structure analysis gave an ortho-

rhombic symmetry with  $a = 19.7474(2)$  Å,  $b = 5.9006(1)$  Å and  $c = 10.5773(1)$  Å. The final  $R_{\text{Bragg}}$  value in space group  $Pnma$  (62) was 1.0%. The structure can be described by layers of a metal and iodine arrangement forming almost pentagonal holes. Raman measurements were correlated with the two  $\text{IO}_6$  octahedra. Two further barium periodate patterns were observed and indexed.

### Introduction

We recently reported the high temperature synthesis and structure analysis of  $M_2\text{NaIO}_6$  ( $M = \text{Ca, Sr, Ba}$ ) from conventional laboratory X-ray diffraction data.<sup>[1]</sup> These compounds can also be prepared by a co-precipitation method in de-ionized water at room temperature. On heating of the dried precipitations, some of the barium samples with substoichiometric amount of  $\text{Na}^+$  showed  $\text{Ba}_5\text{I}_2\text{O}_{12}$  as impurity. The corresponding rubidium compound could not be prepared by these methods. Instead, on heating, the formation of  $\text{Ba}_5\text{I}_2\text{O}_{12}$  was observed. This observation led to an in-depth study of synthesis, crystal growth, and structural analysis of  $\text{Ba}_5\text{I}_2\text{O}_{12}$ . This compound has been known since 1879 from the reaction:<sup>[2]</sup>



In 1966, the unindexed XRD pattern was published<sup>[3]</sup> and found to be similar to our diffraction patterns. To date, no structural data on  $\text{Ba}_5\text{I}_2\text{O}_{12}$  have been available.

In the past few years, several methods have been developed to solve structures from powder samples<sup>[4]</sup> using reciprocal space methods (charge flipping, Patterson, Multan...)<sup>[5–7]</sup> or real space methods (FOX).<sup>[8]</sup> Diffraction patterns from conventional laboratory data are nowadays reliable enough to solve and analyze even complicated unknown structures. Herein, however, the powder quality (average crystallite size or coherence length) is important in order to obtain a reasonably well resolved diffraction pattern.

### Results and Discussion

A crystalline powder of  $\text{Ba}_5\text{I}_2\text{O}_{12}$  with a coherence length of ca. 100 nm in diameter was obtained by adding  $\text{Rb}_2\text{O}$  as a mineralizer to an amorphous precipitate from solutions of  $\text{Ba}(\text{OH})_2 \cdot 8\text{H}_2\text{O}$  and  $\text{H}_5\text{IO}_6$ . After drying, this amorphous powder was heated up to ca. 700 °C. DSC measurements revealed three endothermic signals at 370 °C, 500 °C, and 550 °C (onset points), suggesting the formation of three different compounds. The XRD patterns of these three distinct compounds were indexed with a LSI subroutine included in the program package TOPAS<sup>[9,10]</sup> and gave an orthorhombic, a hexagonal, and an orthorhombic unit cell (title compound, Figure 1). The lattice parameters and possible space groups for the two first compounds are given in Table 1. The structure analysis of the second structure is advanced.

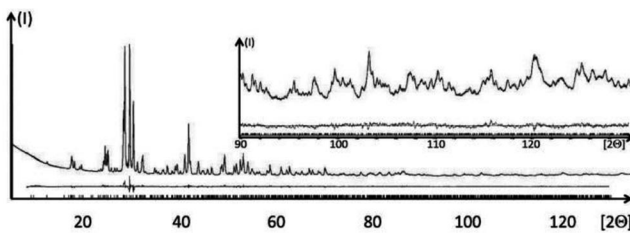


**Figure 1.** Observed, calculated, and difference  $\text{CuK}_{\alpha 1,2}$  - XRD pattern for  $\text{Ba}_5\text{I}_2\text{O}_{12}$  determined by Rietveld refinement using the TOPAS program.<sup>[9]</sup> Intensities between 90 and 130° are increased by a factor of 20.

**Table 1.** Lattice parameters and possible space groups for two unknown barium periodates.

400 °C	<i>Pnma</i>	500 °C	<i>P6<sub>3</sub>/mmc</i>
<i>a</i> /Å	7.466 (1)	<i>a</i> /Å	5.977(1)
<i>b</i> /Å	5.938(1)	<i>c</i> /Å	14.361(3)
<i>c</i> /Å	21.46(1)	<i>R</i> <sub>Bragg</sub> /%	1.16
<i>R</i> <sub>Bragg</sub> /%	0.34	<i>R</i> <sub>Bragg</sub> /%	

\* Univ.-Prof. Dr. F. Kubel  
Fax: +43-1-58801-17199

E-Mail: Frank.Kubel@tuwien.ac.at

[a] Institute of Chemical Technologies and Analytics  
Getreidemarkt 9/164-SC,  
1060 Vienna, Austria

[b] Department of Physical Chemistry,  
University of Geneva  
30, quai E. Ansermet, 1211  
Geneva 4, Switzerland

Several attempts to grow single crystals of the title compound were unsuccessful, but the powder quality had to be improved to be suitable for powder XRD analysis. The powder resulting from the reaction of  $\text{BaI}_2$  in air presents an average crystal size of ca. 60 nm, which is too small for a satisfactory structure solution. As a mineralizer, rubidium ion was found to be helpful to increase the crystal size. Small amounts of  $\text{Rb}^+$  improved the crystal growth slightly. Finally, an almost single phase powder of  $\text{Ba}_5\text{I}_2\text{O}_{12}$  was obtained with an average coherence length of ca. 120 nm.<sup>[19]</sup> This sample was found to be suitable to solve the structure from conventional powder diffraction data.

Indexing the 25 first reflections<sup>[10]</sup> (see Figure 1) gave an orthorhombic unit cell. A whole pattern fitting using the Le Bail method,<sup>[11]</sup> after crystallographic transformations, suggested the space group  $Pnma$  as the one with the highest possible symmetry. The structure was solved in this space group by using the FOX program package,<sup>[8]</sup> as described in the Experimental Section. The starting model was based on five barium ions and two rigid  $\text{IO}_6$  octahedra. After convergence, the structure was refined with TOPAS (see Figure 1). The refinement parameters are summarized in Table 2 for 34 atomic coordinates and 3 isotropic temperature coefficients. Structural data are given in Table 3 and selected interatomic distances are given in Table 4 together with the calculated valence bond sum.<sup>[12,13]</sup> The values for Ba scatter between 1.6 and 2.7. The unusual high valence bond sum (VBS) of Ba2 is probably related to the lowest coordination number 7 and short Ba–O distances. In difference to the other Ba ions in the structure, Ba2 is located in a tunnel-shaped arrangement of oxygen atoms parallel to the  $b$  axis. The high VBS value marks probably the

**Table 2.** Experimental details of the crystal structure determination of the  $\text{Ba}_5\text{I}_2\text{O}_{12}$ , e.s.d.'s of the last digits in parenthesis.

Formula	$\text{Ba}_5\text{I}_2\text{O}_{12}$
Molar mass /g·mol <sup>-1</sup>	1132.45
Crystal system	orthorhombic
Space group	$Pnma$ (No. 62)
Temperature /K	293
$a$ /Å	19.7473(2)
$b$ /Å	5.9006(1)
$c$ /Å	10.5773(1)
Unit cell volume /Å <sup>3</sup>	1232.47(2)
Cell formula units $Z$	4
Density /g·cm <sup>-3</sup>	6.103
Radiation wavelength /Å	1.5418
$\mu(\text{Cu}-K_{\alpha})$ /mm <sup>-1</sup>	162.3
Ø Crystallite size /nm	110(1)
2 theta min /°	5
2 theta max /°	135
2 increment in theta /°	0.02
Number of data points	6500
Number of reflections	576
$hkl$	0.18; 0.5; 0.9
Number of variables	58
$R_F$ /%	2.7
$R_w$ /%	3.6
$R_w$ expected /%	1.3
$R_{\text{Bragg}}$ /%	1.0
Goodness of fit	2.9
ICSD No.	426639

limit of the stability of this structure. The VBS values for iodine are in the expected range (Table 4). Figure 2a shows the structural arrangement perpendicular to the  $b$  axis and Figure 2b the oxygen channel around Ba2. The structure can be described by cations forming a two-dimensional network around an almost pentagonal hole, which is covered by the layers above and below. Oxygen atoms O5–O8 are located within the layer and oxygen atoms O1–O4 connect the different layers. All oxygen atoms are part of the two  $\text{IO}_6$  octahedra. The average Ba–O distance is 2.89(1) Å, the shortest distance Ba3–O8 was calculated to be 2.54(1) Å. Similar short distances were found in  $\text{Ba}_4\text{I}_6\text{O}$ ,  $\text{Ba}_2\text{I}_2\text{O}$ , and  $\text{BaI}_2\text{O}_6$ .<sup>[14–16]</sup> Coordination numbers (and average distances) are 7 for Ba2 (2.64 Å), 10 for Ba1 (2.93 Å), Ba3 (2.89 Å), and Ba4 (2.87 Å) and 11 for Ba5 (3.02 Å). It should be noted that the coordination number of 7 around Ba2 is unexpected. Nevertheless a geometrically similar environment was observed around zirconia

**Table 3.** Standardized atomic positions and  $U_{\text{iso}}$  ( $\times 100$ ) for  $\text{Ba}_5\text{I}_2\text{O}_{12}$  with estimated standard deviations in parentheses.

Atom	$x$	$y$	$z$	$U_{\text{iso}} \times 100$ /Å <sup>2</sup>
Ba1	0.04848(10)	1/4	0.08946(19)	1.32(3)
Ba2	0.14076(9)	1/4	0.38362(16)	1.32(3)
Ba3	0.19920(8)	1/4	0.7409(2)	1.32(3)
Ba4	0.34355(10)	1/4	0.47474(16)	1.32(3)
Ba5	0.42808(9)	1/4	0.08870(19)	1.32(3)
I1	0.01318(10)	1/4	0.7492(2)	0.85(4)
I2	0.23962(11)	1/4	0.1007(2)	0.85(4)
O1	0.0427(6)	0.5255(19)	0.3291(12)	2.90(12)
O2	0.1882(7)	0.007(2)	0.1828(13)	2.90(12)
O3	0.2887(6)	0.019(2)	0.0210(12)	2.90(12)
O4	0.4400(7)	0.524(2)	0.3268(14)	2.90(12)
O5	0.0733(8)	1/4	0.6055(18)	2.90(12)
O6	0.3046(7)	1/4	0.2409(18)	2.90(12)
O7	0.4556(8)	1/4	0.5999(18)	2.90(12)
O8	0.6783(8)	1/4	0.5220(17)	2.90(12)

**Table 4.** Selected interatomic distances for  $\text{Ba}_5\text{I}_2\text{O}_{12}$  with estimated standard deviations in parentheses. The bond valence sum (BVS) in curly brackets is calculated with Platon.<sup>[12,13]</sup>

Atom	Atom (z)	Distance	Atom	Atom (z)	Distance
Ba1	O7	2.716(18)	Ba4	O7	2.578(17)
{1.8}	O8	2.821(17)	{2.3}	O6	2.590(19)
	O4(2 ×)	2.824(13)		O2(2 ×)	2.746(14)
	O7(2 ×)	2.9534(8)		O4(2 ×)	2.947(13)
	O1(2 ×)	3.013(12)		O8(2 ×)	2.982(2)
	O4(2 ×)	3.091(14)		O3(2 ×)	3.096(12)
Ba2	O3(2 ×)	2.565(13)	Ba5	O1(2 ×)	2.919(12)
{2.7}	O1(2 ×)	2.593(12)	{1.6}	O6	2.921(16)
	O5	2.699(18)		O5(2 ×)	2.9558(12)
	O2(2 ×)	2.728(14)		O4(2 ×)	3.001(14)
Ba3	O8	2.542(18)		O1(2 ×)	3.103(13)
{2.2}	O2(2 ×)	2.762(13)		O3(2 ×)	3.153(12)
	O3(2 ×)	2.827(13)			
	O5	2.869(16)			
	O6(2 ×)	2.9513(4)			
	O4(2 ×)	3.189(13)			
I1	O4(2 ×)	1.820(13)	I2	O8	1.776(17)
{6.7}	O1(2 ×)	1.913(12)	{6.6}	O3(2 ×)	1.871(13)
	O5	1.928(18)		O6	1.961(17)
	O7	1.960(18)		O2(2 ×)	1.959(13)

nium in monoclinic  $ZrO_2$ .<sup>[17]</sup> The average I–O distances of the  $IO_6$  octahedra are 1.87 and 1.91 Å, as observed for other periodates.<sup>[1]</sup>

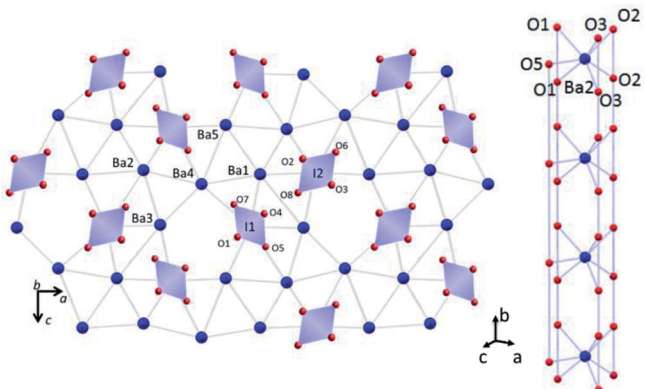


**Figure 2.** A layer of barium and  $IO_6$  octahedra in  $Ba_5I_2O_{12}$  (a), and a channel-type arrangement around  $Ba_2$  (b). Blue atoms: barium, blue polyhedra with iodine in the center, small red atoms: oxygen. The layer is perpendicular to the image given in the Table of Contents.

The Raman spectrum (see Figure 3) confirms the previously reported data<sup>[18]</sup> and is consistent with two  $IO_6$  units with orthorhombic symmetry. The two strong bands at 716 and 685 cm<sup>-1</sup> can be assigned to the totally symmetrical stretching mode ( $A_g$  component) of the  $IO_6$  octahedron. Further, the two weaker bands at 703 and 664 cm<sup>-1</sup> could correspond to the factor group split components (with  $B_{1g}$  symmetry) of the same totally symmetrical stretching mode (of the isolated  $IO_6^{5-}$  ion). Considering the previously calculated stretching frequencies using DFT methods for the isolated  $IO_6$  octahedron,<sup>[1]</sup> the average I–O bond length can be estimated to differ by about 0.012 Å for the two octahedra. This difference is smaller than the observed one (0.04 Å), but it is important to consider that the standard deviations for the refined bond lengths range from 0.012 to 0.018 Å.

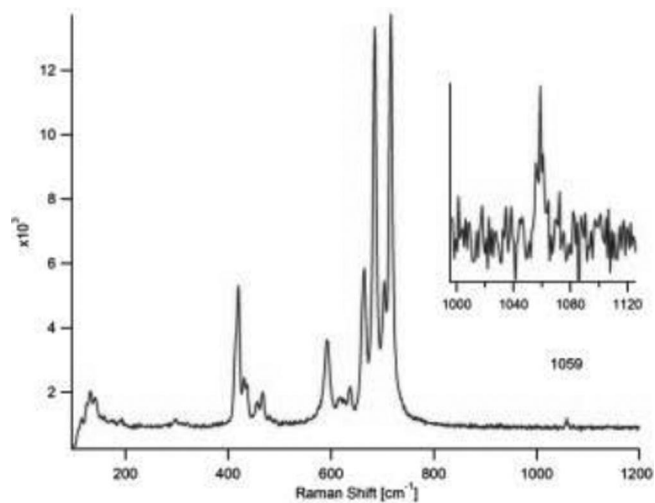


**Figure 3.** Raman spectrum of  $Ba_5I_2O_{12}$  (see also reference<sup>[18]</sup>).

The presence of OH<sup>-</sup> groups can also be observed using IR spectroscopy. In the paper by Siebert,<sup>[18]</sup> no such band was reported for the title compound, and our Raman spectrum is in

perfect agreement with the Raman spectrum reported in this paper for the same compound. In Raman spectroscopy, these OH bands are much weaker.<sup>[19]</sup> A careful inspection of our Raman spectrum reveals a very weak band at 1059 cm<sup>-1</sup>, which potentially could correspond to an OH bond, however its linewidth (ca 8 cm<sup>-1</sup>) is smaller than those of the OH bands in  $BaH_4I_2O_{10}$ . It is much more likely that this band corresponds to a small  $BaCO_3$  impurity (literature value 1060 cm<sup>-1</sup>).<sup>[20]</sup> XRD refinements gave maximal 0.6(1) wt-% of nanocrystalline  $BaCO_3$ . Structural parameters of  $Ba_5I_2O_{12}$  are not changed significantly after this refinement. As can be seen on Figure 3, we do not observe any other band between 1000 and 1200 cm<sup>-1</sup>, which could correspond to an OH bond.

## Conclusions

Laboratory X-ray diffractometer provide data that are good enough to obtain structural parameters, as shown in the example of  $Ba_5I_2O_{12}$ . The possibility to solve ab initio structures from powder diffraction data should not distract from a great number of problems. The quality of the crystalline powder, mainly the coherence length, is crucial to obtain suitable patterns. Powders with coherence length of ca. 100 nm for the crystals are in the lower range of possible candidates for ab initio XRD structure analysis. If the crystals are too small, chemists must make an effort at trying crystal growth techniques using mineralizers or stabilizers at the risk of introducing impurities. A bottleneck is the indexing stage that often requires a trial and error approach. Too many or too few reflections lead to no results. Unambiguously determining unit cell and likely space groups requires experience supported by high resolution diffraction patterns and (new) robust indexing strategies. The number of degrees of freedom in the refinement may then give a limit to the complexity of systems. The type of optimization algorithm in real and reciprocal space – nowadays available – needs a reduction in the range of parameter space. Rigid bodies in real space help solve the structure and during a refinement without constraints indicate the robustness of a model.

## Experimental Section

**Synthesis:**  $Ba_5I_2O_{12}$  can be prepared by different methods. The simplest method is the thermal decomposition of  $BaI_2$ .<sup>[1]</sup> The reaction of  $BaI_2$  in air at 650 °C is quantitative. From  $Ba(OH)_2 \cdot 8H_2O$  and  $H_5IO_6$  (in molar ratio of 5:3, both dissolved in water and then mixed) a precipitate was formed. The precipitate was decanted and washed once with distilled water. About 50 mg of  $Rb_2O$  were added to approximately 2 g of the still wet precipitate. This mixture was allowed to dry at 200 °C. XRD analysis gave a pattern of an amorphous powder. The powder was heated at 700 °C to form  $Ba_5I_2O_{12}$ . The heating procedure was also followed by DSC analysis. At 370 °C an endothermic DSC signal was observed and the XRD pattern of this phase was recorded. After subsequent heating at 500 °C, a different crystalline powder – DSC signal at 520 °C – was obtained, which transforms finally above 550 °C to the compound showing the pattern of  $Ba_5I_2O_{12}$ . The pattern with the best resolution was obtained, when small amounts of  $Rb_2O$  were used as a mineralizer.

**Analysis:** The XRD pattern were collected with a PANalytical X'Pert PRO system, recently calibrated and optimized using a NIST-LaB<sub>6</sub>

standard (emission profile, instrument function, tube tails), with primary and secondary Soller slits of 0.04 rad, a fixed divergence slit of 0.5°, a fixed antiscatter slit of 1° and a 200 mm goniometer radius. Silicon zero background platelets for flat samples were used. Measuring time: 360 min, 5–135° in  $2\Theta$ ,  $\text{Cu}-K_{\alpha}$  radiation, ( $\lambda = 1.5418 \text{ \AA}$ ), X'Celerator detector with  $\text{Ni}-K_{\beta}$  filter, and scan length of ca. 2.55°. Raman measurements were made with a Renishaw Raman microscope using 532 nm laser excitation as well as with a system consisting of a 488 nm laser, a Kaiser Holospec monochromator and a liquid nitrogen cooled CCD camera. Energy Dispersive X-ray (EDX) measurement were made with a FEI Quanta 200.

**Structure Analysis:** The EDX analysis in Figure 4 shows of the sample obtained at 500 °C. Only insignificant amounts of rubidium were detected at this stage. Further heating of this sample gave  $\text{Ba}_5\text{I}_2\text{O}_{12}$  with an improved coherence length of 110(1) nm. Under the same synthesis conditions  $\text{BaI}_2 \cdot 2\text{H}_2\text{O}$  decomposes to  $\text{Ba}_5\text{I}_2\text{O}_{12}$  with 85(1) nm. No significant unit cell volume difference was found: 1232.47(2) vs. 1232.70(6)  $\text{\AA}^3$ . Substantial replacement of  $\text{Rb}^+$  ( $r^{\text{CN XI}} = 1.69 \text{ \AA}$ ) /  $\text{OH}^-$  with larger radii against  $\text{Ba}^{2+}$  ( $r^{\text{CN XI}} = 1.57 \text{ \AA}$ ) /  $\text{O}^{2-}$  can therefore be excluded as the  $\text{OH}^-$  and  $\text{O}^{2-}$  radii with values of 1.34  $\text{\AA}$  and 1.36  $\text{\AA}$  differ only slightly.<sup>[21]</sup> The absence of rubidium on barium sites is further confirmed by the XRD refinement; all Ba population values were refined between 1.00(1) and 1.04(1) and were therefore fixed at 1.0. For this reason, only barium iodine and oxygen were refined.

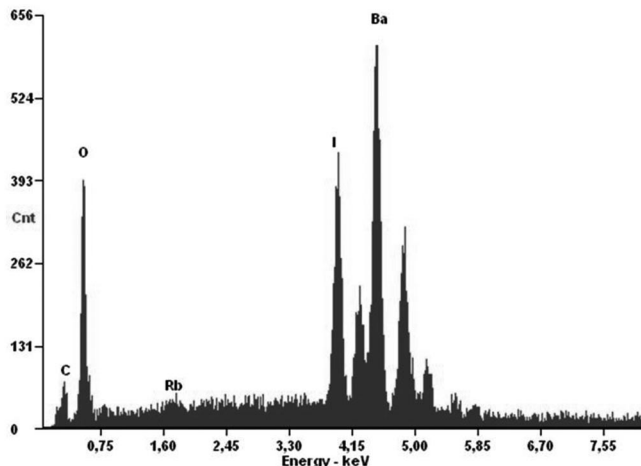


**Figure 4.** EDX analysis from the intermediate sample heated at 500 °C. Only insignificant amounts of  $\text{Rb}^+$  were detected.

The space group of the orthorhombic crystal system of  $\text{Ba}_5\text{I}_2\text{O}_{12}$  with the highest possible symmetry was found from the Le Bail fit procedure ( $R_p = 2.7$  and  $R_{\text{Bragg}} = 0.1\%$ ). Space group  $Pnma$  (62) was retained. Raman measurement suggested 2 different  $\text{IO}_6$  groups, so five  $\text{Ba}^{2+}$  ions are needed. A unit cell volume of 1232.47(2)  $\text{\AA}^3$  was expected to hold four  $\text{Ba}_5\text{I}_2\text{O}_{12}$  units in order to obtain a reasonable density. Based on possible density calculations, the Raman analysis and the stoichiometry, five individual  $\text{Ba}^{2+}$  positions and two  $\text{IO}_6$  units were used as a starting model for the calculation in the real space structure solution package FOX.<sup>[18]</sup> The two  $\text{IO}_6$  octahedra were allowed to rotate and move as rigid bodies. The heavy elements converged after some optimization steps towards special Wyckoff positions 4(c) and were subsequently fixed at these positions. The structure then converged to a reasonable arrangement. The evaluation and Rietveld refinement with the fundamental parameters approach were performed with the TOPAS<sup>[19]</sup> software. Refined parameters included 6 background coefficients (for Chebyshev polynomials), lattice param-

eters, strain, crystallite size, zero point, sample absorption, positional parameters, and constrained vibrational parameters. Crystallite size, coherence length, and particle size has an effect on powder X-ray reflections. Brindley<sup>[22]</sup> describes this effect in relation to the quantitative determination of crystalline substances. No constraints on positions were necessary. Finally, the good quality of the diffraction pattern also at high angle allowed varying the positions of the light atoms (oxygen) during the refinement procedure.

Further details of the crystal structure investigations may be obtained from the Fachinformationszentrum Karlsruhe, 76344 Eggenstein-Leopoldshafen, Germany (Fax: +49-7247-808-666; E-Mail: crysdata@fiz-karlsruhe.de, [http://www.fiz-karlsruhe.de/request\\_for\\_deposited\\_data.html](http://www.fiz-karlsruhe.de/request_for_deposited_data.html)) on quoting the depository number CSD-426639.

## Acknowledgements

The X-ray center of the Vienna University of Technology is acknowledged for providing access to the powder diffractometer. The authors want to thank *Dr. Erich Halwax* (TU Wien) for helpful discussions and *Elisabeth Eitenberger* for EDX measurements. This work was supported in part by the Swiss National Science Foundation.

## References

- [1] F. Kubel, N. Wandl, M. Pantazi, V. D'Anna, H. Hagemann, *Z. Anorg. Allg. Chem.* **2013**, *6*, 892–898.
- [2] S. Sugiura, C. F. Cross, *J. Chem. Soc. Trans.* **1879**, *35*, 118–119.
- [3] B. Frit, B. Tanguy, P. Hagenmuller, *Bull. Soc. Chim. Fr.* **1966**, *7*, 2190–2193.
- [4] H. Putz, J. C. Schön, M. Jansen, *J. Appl. Crystallogr.* **1999**, *32*, 864–870.
- [5] C. Baerlocher, F. Gramm, L. Massüger, L. B. McCusker, Z. He, S. Hovmöller, X. Zou, *Science* **2007**, *315*, 1113–1116.
- [6] P. Main, S. J. Fiske, S. E. Hull, L. Lessinger, G. Germin, J. P. Declercq, M. M. Woolfson, *MUL TAN-80, A System of Computer Programs for the Automatic Solution of Crystal Structures from X-ray Diffraction Data*, University of York, UK, **1980**.
- [7] A. L. Patterson, *Phys. Rev.* **1934**, *46*, 372–376.
- [8] V. Favre-Nicolin, R. Cerny, *J. Appl. Crystallogr.* **2002**, *35*, 734–743.
- [9] TOPAS, Version 4.2, Bruker AXS GmbH, Karlsruhe, Germany, **2009**.
- [10] A. A. Coelho, *J. Appl. Crystallogr. A* **2003**, *32*, 86–95.
- [11] A. Le Bail, *Powder Diffract.* **2005**, *20*, 316–326.
- [12] A. L. Spek, *J. Appl. Crystallogr.* **2003**, *36*, 7–13.
- [13] N. E. Brese, M. O'Keeffe, *Acta Crystallogr., Sect. B* **1991**, *47*, 192–197.
- [14] M. G. Barker, M. G. Francesconi, C. Wilson, *Acta Crystallogr. Sect. E* **2001**, *57*, 41–43.
- [15] O. Reckeweg, F. J. DiSalvo, *Z. Naturforsch.* **2008**, *63b*, 519–524.
- [16] V. Petricek, K. Maly, B. Kratochvil, J. Podlahova, J. Loub, *Acta Crystallogr., Sect. B* **1980**, *36*, 2130–2132.
- [17] R. J. Hill, L. M. D. Cranswick, *J. Appl. Crystallogr.* **1994**, *27*, 802–844.
- [18] H. Siebert, G. Wieghardt, *Z. Naturforsch.* **1972**, *27b*, 1299–1304.
- [19] H. Haeusler, M. Wagener, *J. Mol. Struct.* **2008**, *892*, 1–7.
- [20] I. A. Degen, G. A. Newman, *Spectrochim. Acta A* **1993**, *49*, 859–887.
- [21] R. D. Shannon, *Acta Crystallogr., Sect. A* **1976**, *32*, 751–767.
- [22] G. W. Brindley, *Phil. Mag.* **1945**, *36*, 347–369.

Received: April 30, 2014  
Published Online: August 6, 2014